Relative contribution of surface mass balance and ice flux changes to the accelerated thinning of the Mer de Glace (Alps) over 1979-2008

Etienne Berthier, Christian Vincent

Relative contribution of surface mass balance and ice flux changes to the accelerated thinning of the Mer de Glace (Alps) over 1979-2008

Etienne Berthier[1] & Christian Vincent[2]

[1]*CNRS, Université de Toulouse, LEGOS, 14 avenue Edouard Belin Toulouse 31400 France*
[2]*CNRS – Université Grenoble 1, LGGE, 54 rue Molière, BP 96, F-38402 Saint Martin d'Hères Cedex, France*

Accepted for publication in the ***Journal of Glaciology*** *(http://www.igsoc.org/journal/)*

Abstract

By subtracting surface topographies from 1979, 1994, 2000 and 2008, we measured ice thinning rates increasing from 1 m a^{-1} (1979-1994) to more than 4 m a^{-1} (2000-2008) on the tongue of the Mer de Glace. The relative contributions of changes in surface mass balance and ice fluxes to this acceleration in the thinning are estimated using field and remote sensing measurements. Between 1979-1994 and 2000-2008, surface mass balance diminished by 1.2 m w.e. a^{-1} mainly because of atmospheric warming. Mass balance changes induced by the growing debris-covered area and the evolving glacier hypsometry compensated each other. Meanwhile, the Mer de Glace slowed down and the ice fluxes through two cross-sections at 2200 m a.s.l. and 2050 m a.s.l. decreased by 60%. Between 1979-1994 and 2000-2008, two thirds of the increase in the thinning rates was caused by reduced ice fluxes and one third by rising surface ablation. However, those numbers need to be interpreted cautiously given our inability to respect mass conservation below our upper cross section. An important implication is that large errors would occur if one term of the continuity equation (e.g., surface mass balance) was deduced from the two others (e.g., elevation and ice flux changes).

1. Introduction

The sensitivity of glacier mass balance to climate change is widely recognized (Dyurgerov and Meier, 1999; Lemke and others, 2007; Oerlemans, 2001; Ohmura, 2006; Vincent, 2002). In a warming climate, a consequence of this sensitivity is a rapid thinning of most glaciers, in particular at their lowest elevations (Schwitter and Raymond, 1993). Over the last decades, this thinning has been observed for most mountain glacier tongues using either field measurements (e.g., Vincent and others, 2009) or various remote sensing techniques (e.g., Berthier and others, 2010; Kohler and others, 2007; Magnússon and others, 2005; Nuth and others, 2010; Paul and Haeberli, 2008; Rignot and others, 2003; Soruco and others, 2009; Surazakov and Aizen, 2006).

The continuity equation, applied to a glacier tongue, indicates that two main processes potentially drive this recent low elevation thinning (Cuffey and Paterson, 2010; Nuth and others, 2012): (i) a warmer climate leads to an enhanced ablation at the glacier surface (Vincent and others, 2004); (ii) decreasing ice fluxes from upstream regions can also play a role. For mountain glaciers, a contribution of ice dynamics to their recent low elevation thinning is often suggested (Lambrecht and Kuhn, 2007; Paul and others, 2007; Rignot and others, 2003), but quantified in only few studies (Hagen and others, 2005; Huss and others, 2007; Vincent and others, 2009). In particular, Huss et al. (2007) showed that present-day ice fluxes from the upper part of Unteraargletscher (Swiss Alps) are insufficient to counteract the high ablation rates on the glacier tongue and, in their effort to model future retreat scenario, highlighted the importance of taking into account an evolving ice dynamics. On Argentière Glacier (French Alps), Vincent and

others (2009) also showed that the elevation changes below 1800 m are mainly dynamically-driven. Located close to Argentière Glacier, the tongue of the Mer de Glace has also experienced an accelerated thinning in the late 20th and early 21st century (Berthier and others, 2004). The first goal of the present paper is to quantify the relative contribution of changes in surface mass balance and changes in glacier dynamics (ice fluxes) to this accelerated thinning.

Additionally, an important question in modern glaciology is to determine whether it is reasonable to infer area-averaged surface mass balance changes of a glacier tongue from observations of the thinning rates and the ice fluxes only. This question deserves attention given that surface mass balance (and its temporal variations) is the glacier variable more closely related to climate change (e.g., Vincent and others, 2004). The spatial pattern of surface mass balance of a limited number of glacier tongues can be measured directly from field measurements using ablation stakes but cannot be directly measured regionally from remote sensing methods (photogrammetry, laser scan or satellite images). Thus, deriving this variable for large, remote, numerous and/or debris-covered glacier tongues remains problematic.

In the past, there has been various attempts to infer the spatial distribution of mountain glacier surface mass balance from (i) the principle of mass conservation combined with remotely-sensed elevation changes and a well-constrained high-resolution ice flow model (Hubbard and others, 2000) or (ii) the kinematic boundary condition applied to a glacier tongue and constrained using remotely-sensed surface elevation changes and velocities (Gudmundsson and Bauder, 1999; Kääb and Funk, 1999; Kääb, 2000). In both cases, comprehensive bedrock topographies were required. Hubbard and others (2000) were successful in modeling the annual mass balances measured at ablation stakes at Haut Glacier d'Arolla (Swiss Alps) but the obvious drawback of their method is the difficult transferability to other glaciers that may not present a simple geometry and/or not be as extensively monitored as Haut Glacier d'Arolla. An alternative to these complex and data demanding approaches is to infer the average surface mass balance below (or between) selected cross sections where the bedrock topography is known (Reynaud and others, 1986). The latter approach does not provide the complete spatial distribution of glacier mass balance, but it is simpler and less data-demanding, thus easier to apply to remote or larger glaciers. This cross-section approach has received renewed attention recently to derive tongue-wide average mass balance and its change with time, in particular for Himalayan/Tibetan partly debris-covered glaciers (Nuimura and others, 2011; Sakai and others, 2006; Zhang and others, 2010). However, the reliability of mass balance changes inferred from this cross-section method has not been assessed using observed values at ablation stakes.

Thus, the second goal of this paper is to test, for the relatively well-observed Mer de Glace tongue, whether it would be reasonable to infer temporal variations in surface mass balance from changes in geometric variables (surface elevation and ice fluxes) only.

2. Thinning of the lower Mer de Glace between 1979 and 2008

The Mer de Glace, the largest glacier in the French Alps with an area of ~30 km^2 (Zumbühl and others, 2008), is located in the Mont-Blanc massif (Figure 1). It is composed of an upper basin whose maximum elevation reaches about 4300 m. From this accumulation region, the ice flows rapidly (maximum surface velocities of 900 m a^{-1} were measured by Reynaud (1973) and 700 m a^{-1} by Berthier and others (2005)) through a narrow and steep portion (the Géant ice fall, between 2700 m and 2400 m) before feeding the lower 7 km of the glacier down to a front located at about 1500 m. During the last fifteen years, the equilibrium line altitude (ELA) has been located above the Géant Ice Fall at an altitude of about 2800 m (Rabatel and others, 2005). The lower part of the glacier tongue is covered with debris. The extent of the debris-covered area is growing since the end of the little ice age (Deline, 2005).

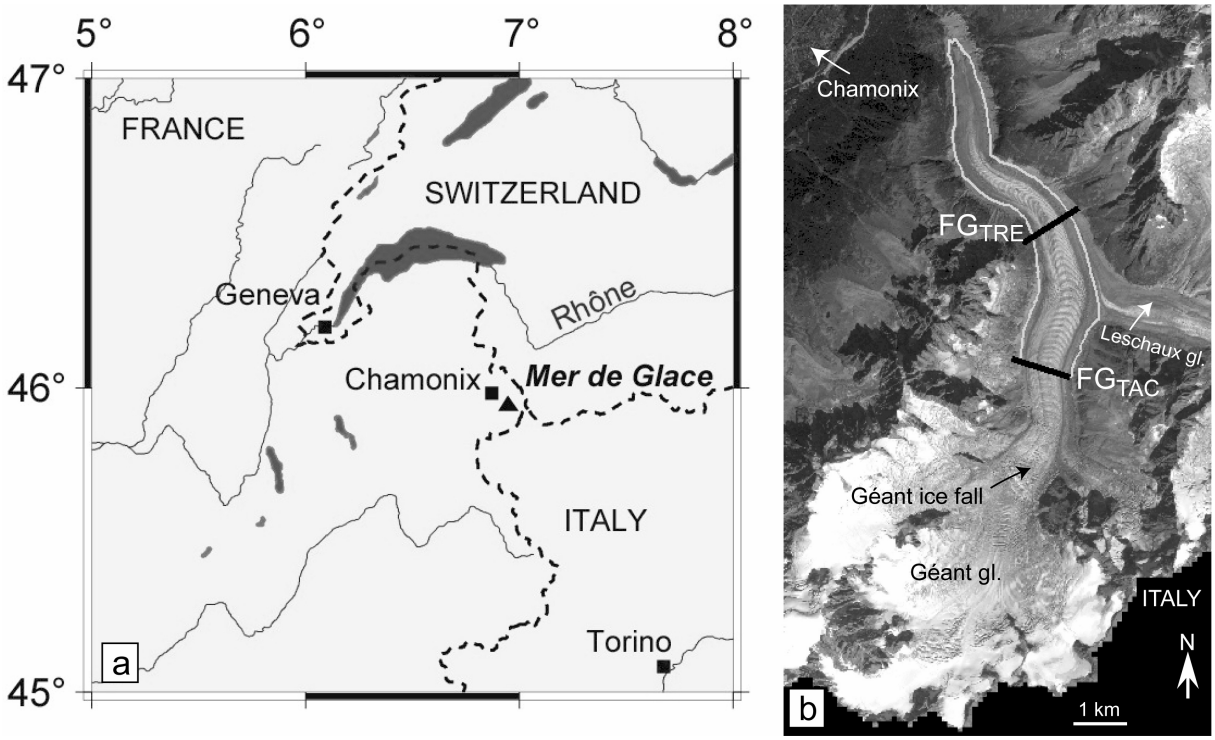

Figure 1: (a) The Mer de Glace (dark triangle) in the Mont-Blanc area of the French Alps, close to the border between France, Switzerland and Italy. (b) Orthorectified SPOT5 image acquired in August 2003 (© CNES 2003 / Distribution Spot Image). The main glacier features are named (gl. stands for glacier). The portion of the Mer de Glace studied here (outlined) is located downstream of two flux gates labelled "FG_{TAC}" (TAC strands for Tacul) and "FG_{TRE}" (TRE stands for Trélaporte).

In a previous study, we have adjusted and compared a 1979 map from the French mapping agency (Institut Géographique National, IGN) and satellite-derived digital elevation models (DEMs) to determine the changes in surface elevation of the Mer de Glace between 1979-1994, 1994-2000 and 2000-2003 (Berthier and others, 2004). The comparison with elevation profiles surveyed in the field each year showed that, after Gaussian filtering and averaging by altitude range, the DEM-derived elevation changes were accurate within ± 1-2 m in the ablation area. One conclusion of our work was that the lower part of the Mer de Glace had been recently thinning at an increasing rate. Here, we have extended our time series by using an additional DEM derived from a SPOT5 2.5-m stereo-pair acquired 26 August and 2 September 2008 (Figure 2). This 2008 DEM is used in place of the 2003 DEM that had a short (3-year) time separation with the previous DEM (2000), resulting in larger uncertainties on the thinning rates.

Between a flux gate (noted FG_{TRE}, Figure 1b) at about 2050 m in 1979 and the glacier front (a glacierized area of about 2 km^2), the average ice thinning rate has evolved from 0.6±0.1 m a^{-1} in 1979-1994 (referred as epoch I in the following) to 3.0±0.3 m a^{-1} in 1994-2000 (epoch II) and 4.0±0.2 m a^{-1} in 2000-2008 (epoch III). In other words, the ice thinning rate has increased by, first, 2.4±0.4 m a^{-1} (from epoch I to II) and then by 1.0±0.4 m a^{-1} (from epoch II to III). Between another flux gate (noted FG_{TAC}, Figure 1b) at higher altitude (about 2225 m in 1979) and the glacier front, the ice thinning rate has increased by 1.7±0.4 m a^{-1} (from epoch I to II) and 1.0±0.4 m a^{-1} (from epoch II to III). The main goal of the present study is to understand what has driven this acceleration of the thinning of the lower Mer de Glace during recent years.

For the portion of the Mer de Glace downstream of a flux gate (FG), the equation of mass conservation (Cuffey and Paterson, 2010; Reynaud and others, 1986) states that the change in surface elevation (h) with time (t) between year 1 (yr1) and year 2 (yr2) is the sum of the area-average surface mass balance (B) and the flux term (all terms in m of ice per year):

$$\left\langle \frac{\delta h}{\delta t} \right\rangle_{yr1-yr2} = \frac{\langle B \rangle_{yr1-yr2}}{\rho} + \left\langle \frac{\Phi_{FG} - \Phi_{front}}{A} \right\rangle_{yr1-yr2} \qquad \text{Eq. 1}$$

Where ρ is the density of ice (900 kg m^{-3}), Φ_{FG} is the ice flux though FG, Φ_{front} is the flux at the glacier front (Φ_{front} = 0) and A is the glacier area below FG. $< >_{yr1\text{-}yr2}$ indicates an average between year 1 and year 2. $\left\langle \frac{\Phi_{FG}}{A} \right\rangle_{yr1-yr2}$ is the average emergence velocity below FG (noted $\bar{V}$) between year 1 and year 2.

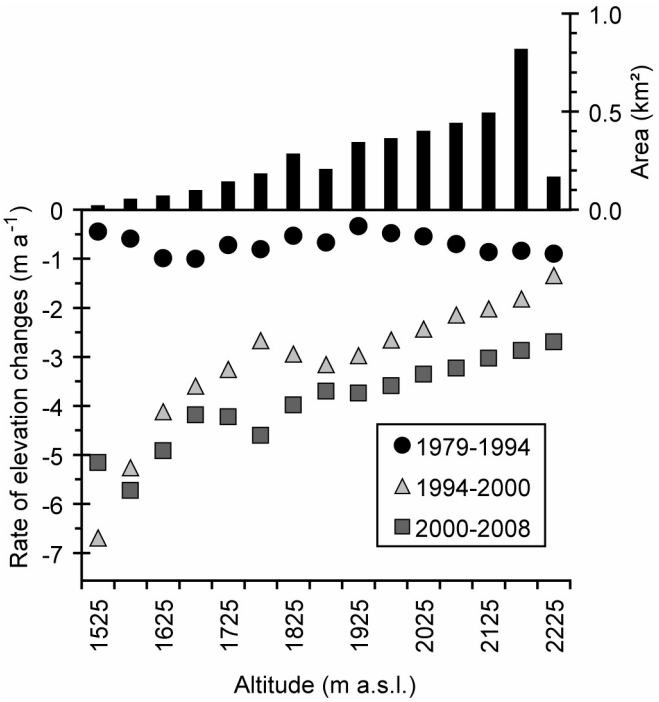

Figure 2: Rate of surface elevation changes as a function of altitude on the Mer de Glace tongue for three different epochs. The upper histogram shows the ice hypsometry below the Tacul flux gate in 1979.

Consequently, to understand the increase in the thinning rate of the lower Mer de Glace from one epoch to another (left hand side term in Eq. 1), we computed the surface mass balance (section 3) and the emergence velocity (section 4) of the glacier tongue for each epoch (I, II and III).

The choice of the flux gates (FG_{TAC} and FG_{TRE}) was constrained by data availability and glaciological reasons. Those flux gates correspond to two of the five transverse profiles where the surface topography is measured yearly in the field with an accuracy of ±0.5 m (Vincent and others, 2009). The upstream flux gate, FG_{TAC}, has the advantage to feed a larger area (about 4 km^2 compared to 2 km^2 for Trélaporte) but it is located above the confluence of the Mer de Glace with Leschaux Glacier (Figure 1b) and we lack thickness and velocity measurements to estimate the ice fluxes coming from this tributary glacier. The three other flux gates, downstream of Trélaporte, are not considered here because they feed a much smaller part (less than 0.7 km^2) of the glacier tongue where only 2 ablation stakes are surveyed each year.

3. Changes in surface mass balance

3.1. Field measurements at ablation stakes

Each year in late September, the annual surface mass balance is determined on the Mer de Glace below 2300 m using an ablation stake network mainly located along the glacier centerline. The annual mass balance varies from about -4 m w.e. a^{-1} at 2300 m to -9 m w.e. a^{-1} at the lowest ablation stake (1750 m). All annual mass balance measurements available on clean ice between hydrological years 1979-1980 and 2007-2008 are processed using the linear mass balance model (Lliboutry, 1974) and are corrected for local elevation changes. This model consists in the linear decomposition of time and space variability of surface mass balance. The surface mass balance at each stake ($b_{i,t}$) is modeled as the sum of its spatial pattern (α_i), its temporal anomalies (β_t) and a residual ($\varepsilon_{i,t}$).

$$b_{i,t} = \alpha_i + \beta_t + \varepsilon_{i,t} \qquad \text{Eq. 2}$$

Details of the method can be found elsewhere (Thibert and Vincent, 2009).

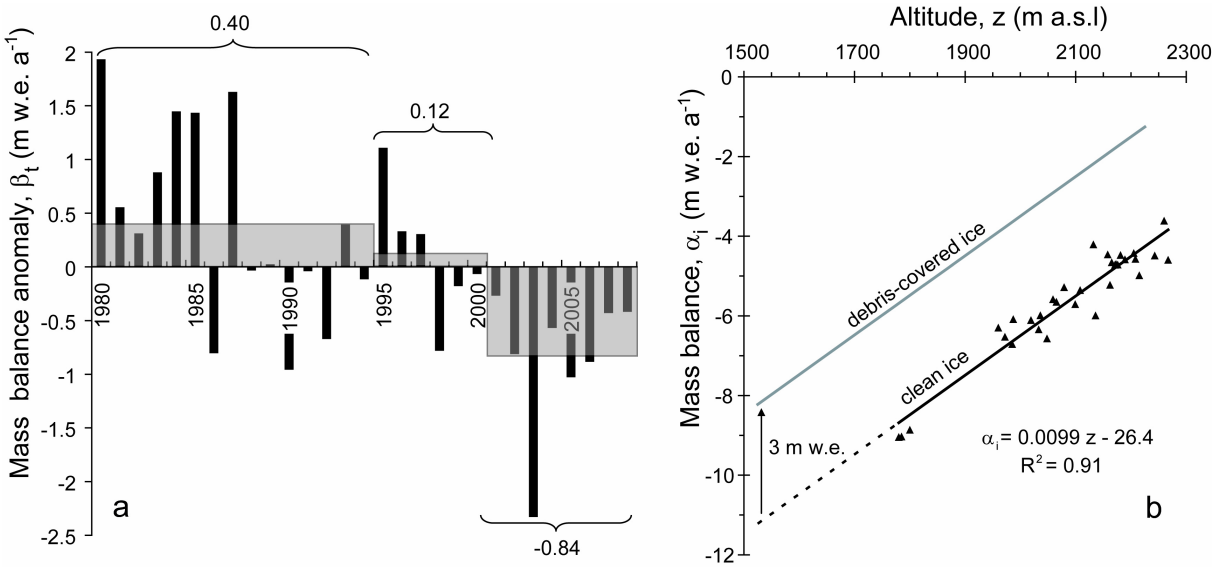

Figure 3: Output of the linear mass balance model (Lliboutry, 1974) applied to all mass balance measurements in the debris-free part of the ablation area of the Mer de Glace between September 1979 and September 2008 (29 hydrological years). (a) Annual mass balance anomaly (β_t). The grey boxes show the mass balance anomalies averaged over epochs I, II and III. (b) Relationship between the 1979-2008 average mass balances (α_i) and altitude (z). The regression lines used on clean and debris-covered ice to compute the mass balance of the whole glacier tongue are also shown.

Over the three time periods considered here (Figure 3a), the mass balance on clean ice has decreased first by 0.28 m w.e. a^{-1} (epoch I to II) and then by 0.96 m w.e. a^{-1} (epoch II to III). From epoch I to III, the total change in mass balance was –1.23 m w.e. a^{-1}. These results are consistent with previous observations on glaciers in the European Alps (Huss and others, 2008; Vincent, 2002; Vincent and others, 2004): the surface mass balance has increased between 1960 and 1981, an increase related to low ablation values. For the more recent period (1982-2008), a sharp mass balance decline is observed and connected to an ablation rise.

3.2. Mass balance for the whole glacier tongue

We now estimate the tongue-averaged mass balance for each epoch, taking into account the evolving hypsometry of the ice-covered area and the reduction of ablation on the debris-covered parts. Lliboutry's linear model provides the mass balances at the location of stakes and, thus, they must be extrapolated to the whole ice tongue. For all stakes (on clean ice), 91% of the mass

balance spatial variance is explained by altitude (Figure 3b). For each epoch, this linear mass balance-altitude relationship is combined with the evolving hypsometry of the debris-free areas to estimate their area-weighted mass balances. For debris-covered areas, the same mass balance gradient with altitude is used but the curve is shifted upward by 3 m w.e. to account for the reduction in ablation due to the insulating effect of debris (Figure 3b). This constant ablation reduction factor under debris (noted f_d) has been estimated from field measurements during 5 years at 5 locations on the Mer de Glace and neighbouring Argentière glacier where ablation was systematically compared between stakes anchored at the same altitude on clean and debris-covered ice (Vincent, 1999). Area-weighted mass balances for the debris-free and debris-covered parts are then summed to obtain the mass balance of the whole glacier tongue. In a final step, we added the mass balance temporal anomaly (β_t) for each epoch. Melt at the base of the glacier was assumed to be negligible.

The hypsometry on the debris-free and debris-covered parts of the glacier is calculated for each year when a DEM is available (1979, 1994, 2000 and 2008). Because we did not have any imagery accompanying the DEM from year 1979, we used instead a SPOT satellite image from 1988 and assumed no change in ice extent between 1979 and 1988, an assumption supported by the limited length variations (only a small advance) during the same time period (Vincent and others, 2007). Between 1988 and 2008, the ice-covered area diminished by 0.4 km^2, mainly close to the glacier front. From visual inspection of the satellite images, the percentage of the glacier tongue covered with debris was digitized and, below FG_{TRE}, found to increase from 45% in 1988 to 65% in 2008 (31% to 45% below FG_{TAC}). Increased ablation due to dust (Oerlemans and others, 2009) and changes in solar radiation due to evolving shading on a lowering glacier surface (Arnold and others, 2006) are not estimated because they should already be accounted for in the mass balance observations at stakes.

During 1979-2008, the average surface mass balance was -6.4 m w.e. a^{-1} below FG_{TRE} and -5.4 m w.e. a^{-1} below FG_{TAC}. Surface mass balance (converted to ice equivalent using a density of 900 kg m^{-3}) for epochs I, II and III are listed in Table 1 (FG_{TAC}) and Table 2 (FG_{TRE}). Interestingly, the mass balance changes between the different periods for the whole tongue are close to the mass balance temporal anomaly (β_t) determined at ablation stakes located on clean ice only. It indicates that the main driver of mass balance change on the Mer de Glace tongue is climate change whereas others feedbacks potentially influencing the mass balance (growing debris coverage, thinning of the tongue and area loss close to the glacier front) nearly compensate each other. Between epoch I and III, the glacier front retreated to higher elevations such that ice-covered areas at the lowermost elevations, where ablation is high, disappeared. Meanwhile, the glacier tongue thinned and, thus, was immerged in a warmer atmosphere due to the adiabatic decrease of temperature with altitude. Those two feedbacks have an opposite effect on ablation (Elsberg and others, 2001) and the net effect is quantified by an average altitude below FG_{TRE} that decreased by 35 m (from 1873 m to 1838 m). This net lowering of the Mer de Glace tongue indicates that, in term of ablation feedbacks, thinning dominates over the retreat of the front. This 35-m area-average lowering corresponds to an enhanced ablation of about 0.35 m w.e. a^{-1} (using the mass balance gradient with altitude from Figure 3b). This increase in ice ablation was counterbalanced by the growth in debris-covered areas (+20% below FG_{TRE}) that lowered the ablation by 0.51 m w.e. a^{-1}.

3.3. Uncertainties on the mass balance

Source of uncertainties on the total mass balance are: (i) the residual, ε_{it}, of the linear mass balance model, ±0.5 m w.e. a^{-1}, that is divided by the square root of the number of years during each period; (ii) the standard deviation, ±0.4 m w.e. a^{-1}, of the residual to the linear fit between mass balance and altitude (Figure 3b). Given the lack of ablation stakes below 1750 m, an extrapolation of the mass balance gradient is needed for the lowermost part of the glacier (dashed line in Figure 3b) where we double the uncertainty to ±0.8 m w.e. a^{-1} ; (iii) the average

altitude of each altitude band is known within ±2 m, translating into a negligible ±0.02 m w.e. a^{-1} mass balance uncertainty; (iv) a ±1 m w.e. a^{-1} uncertainty (33%) was assumed for f_d. This error should account for the unknown spatial variability in debris thickness and only applies to the glacier area covered with debris; (v) a 10% uncertainty was estimated for our ability to delimitate the debris-covered area, and after multiplying by f_d, leads to a ±0.3 m w.e. a^{-1} mass balance uncertainty. Those individual error components are summed quadratically, leading to total uncertainties of, respectively, ±0.8 m w.e. a^{-1} and ±0.7 m w.e. a^{-1} for the area-average surface mass balance below FG_{TRE} and FG_{TAC} (Table 1 and 2).

Lower uncertainties, ±0.4 to ±0.5 m w.e. a^{-1}, are calculated for the mass balance changes from one period to another (Table 1 and 2). This is because the large uncertainty on f_d, ±1 m w.e. a^{-1}, is applied to areas where debris-coverage changed (and not to the total debris-covered area). Also, uncertainties associated to the linear fit of mass balance with altitude (±0.4 m w.e. a^{-1}) are restricted to changing glacier areas (and not to the whole glacier tongue).

4. Changes in ice fluxes and emergence velocities

We now estimate the ice fluxes through both cross-sections for the three different epochs:

$$\Phi_{FG} = \int_S U \, ds = S < U > \qquad \text{Eq. 3}$$

where S represents the area of the cross-section, U is the component of the ice velocity perpendicular to the cross-section and <U> is the depth and width average (=cross-section average) of this velocity component.

4.1. Cross-sectional areas

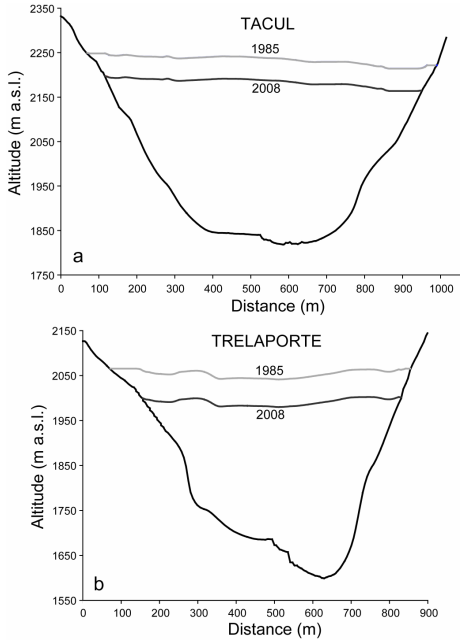

Figure 4: Bedrock (black), 1985 surface (light grey) and 2008 surface (dark grey) elevations at FG_{TAC} (a) and FG_{TRE} (b). Between 1979 and 1985 (not shown), the glacier thickened by 5 m at FG_{TAC} and 10 m at FG_{TRE} before thinning by 50 m at FG_{TAC} and 61 m at FG_{TRE} between 1985 and 2008.

The bedrock topography of the Mer de Glace was measured by various authors (Gluck, 1967; Süsstrunk, 1951; Vallon, 1961) and compiled in a comprehensive map (Lliboutry and Reynaud,

1981). We digitized the elevation contours from this map, interpolated them and then extracted a profile of the sub-glacial topography at FG_{TRE} and FG_{TAC} (Figure 4). To compute the evolving cross-section, the surface elevation is updated using topographic surveys performed yearly (Vincent and others, 2007).

4.2. Surface velocities and their temporal evolution

Velocities are available from two data sources. Spatially sparse but accurate and temporally regular annual velocities are calculated from annual positioning of stakes anchored in the glacier. About 10 to 15 velocity measurements are available each year since 1979 along a longitudinal profile of the Mer de Glace with an accuracy of ±0.2 m a^{-1} (Vincent and others, 2009). The September 1987 survey was not performed which means that velocity data are lacking for hydrological years 1986-87 and 1987-88.

Velocity fields have also been computed by orthorectifying and tracking surface features on 10-m resolution SPOT satellite images. Annual velocity fields are available for hydrological years 1993-1994 and 2000-2001 (Berthier, 2007). The comparison with simultaneous field-derived velocities shows that their precision (1σ) is ±2-3 m a^{-1}, or one quarter of the satellite image pixel size. Two velocity fields, derived from 2.5-m SPOT5 imagery, are also available during summer 2003 with a precision of ±10 m a^{-1} (Berthier and others, 2005).

All velocity measurements are compared along a longitudinal profile (Figure 5). Between 1965 and 1980, inter-annual variations in speed were small, within ±20 m a^{-1} and these fluctuations were in phase all along the longitudinal profile (Lliboutry and Reynaud, 1981). This period was followed first by a small acceleration that peaked in 1985 and then by a strong slowdown.

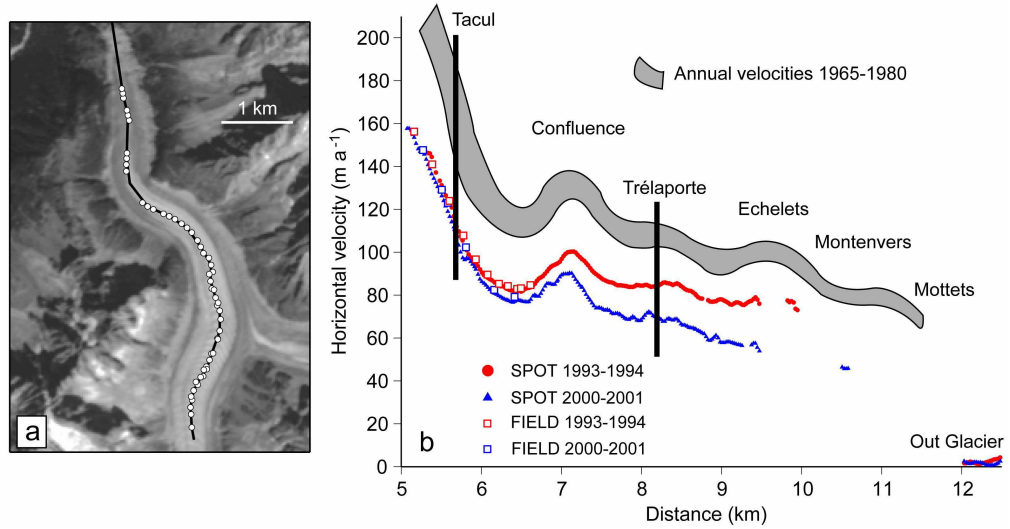

Figure 5. (a) Location of surface velocity measurements along a longitudinal profile of the Mer de Glace (© CNES 2003 / Distribution Spot Image). (b) Changes in annual velocity along this profile. Filled symbols (blue triangles and red dots) correspond to satellite measurements. Other velocities (unfilled red and blue squares and grey envelope) have been measured in the field.

Annual velocities are not available every year at each flux gate exactly, but one velocity measurement is generally available upstream and downstream of the flux gate. Thus, we obtained the velocity at each flux gate by linear interpolation of the surrounding velocities (Figure 6). At FG_{TRE}, the glacier flow has decreased by 52% from a peak velocity of 124 m a^{-1} (hydrological year 1984-85) to a minimum of 59 m a^{-1} (hydrological year 2007-08). At FG_{TAC}, the annual velocity decreased by 49% from a maximum of 180 m a^{-1} in 1980-81 down to 92 m a^{-1} in 2007-08. Since 1984-85, the decrease is nearly linear at FG_{TRE} whereas at FG_{TAC}, there is an 11-

year plateau between 1991-92 and 2002-2003 when velocities remained stable, at about 120 m a^{-1}. Those non monotonic variations in velocity imply that it is important to have continuous, annual velocity measurements to infer realistic multi-year averaged ice fluxes.

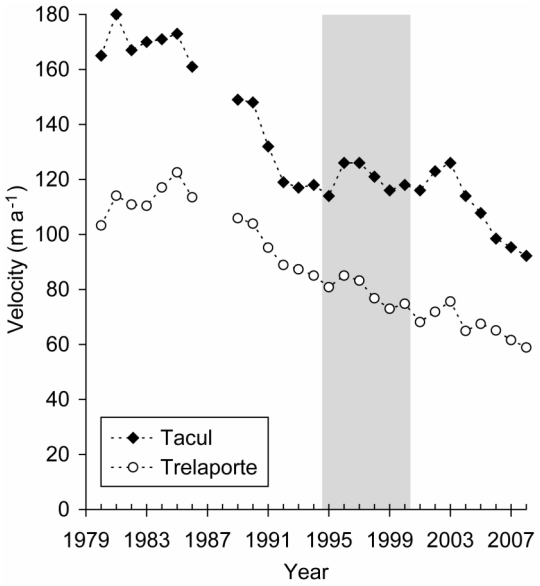

Figure 6: Annual centerline surface velocity at FG_{TRE} (white) and FG_{TAC} (black) between 1979 and 2008. Epoch II (1994-2000) is identified with a grey shading. Data are missing for hydrological years 1986-87 and 1987-88. To estimate the ice fluxes, the velocities for these years were calculated by linear interpolation using the 1985-86 and 1988-89 velocities.

4.3. Changes in ice fluxes

Mean cross-section velocity, <U>, is required to compute the ice fluxes through the flux gates, but only centerline surface velocity ($U_{s,c}$) is available from yearly field measurements. A correcting factor is needed to convert all centerline velocities to mean cross-section velocities.

First, we calculate the ratio between the mean surface velocity for each flux gate, $<U_s>$, and the centerline surface velocity $U_{s,c}$. The ratio is estimated from satellite-derived velocity fields. Preferably, this ratio should be evaluated on annual velocities to limit the influence of seasonal variations in basal sliding (Willis, 1995). The 1993-94 and 2000-01 annual velocity fields do not entirely sample the transverse profile because the tracking of surface features on sequential satellite imagery failed close to the glacier margins where too much shear occurred within one year. Thus, the velocity at the shear margins were filled using linear interpolation between the glacier boundary (where the velocity is 0) and the closest available velocity measurement. At FG_{TRE}, the ratio equals 0.68 in 1993-94 and 0.71 in 2000-01. Additionally, we estimated the ratio on the 2003 summer velocity fields derived from SPOT5 images acquired 19 July-19 August and 23 August-18 September (Berthier and others, 2005). These summer velocity fields have the advantage to provide a complete transverse profile because, after a few weeks, surface features are still trackable even at the shear margins (Figure 7). The ratio equals 0.69 for the August-September velocity field and 0.74 for the July-August velocity field. The average of these 4 values, 0.70 (±0.02), was used to convert all annual centerline velocities to mean surface velocities at FG_{TRE}. At FG_{TAC} (Figure 7c) and using the same procedure, a ratio of 0.8 was calculated between the width-average surface velocity and the centerline surface velocity.

The next step is the conversion from mean surface to depth-averaged velocity. Without basal sliding, theoretical calculations suggest that the depth-averaged velocity is 80% of the surface

velocity (for n = 3 in Glen's law (Cuffey and Paterson, 2010, p 310)). With basal sliding, this percentage increases and, for example, in the case of Athabasca glacier the mean cross-section velocity equals the mean surface velocity (Raymond, 1971). Here, we used an intermediate value assuming that the depth-averaged velocity is 90% of the surface velocity.

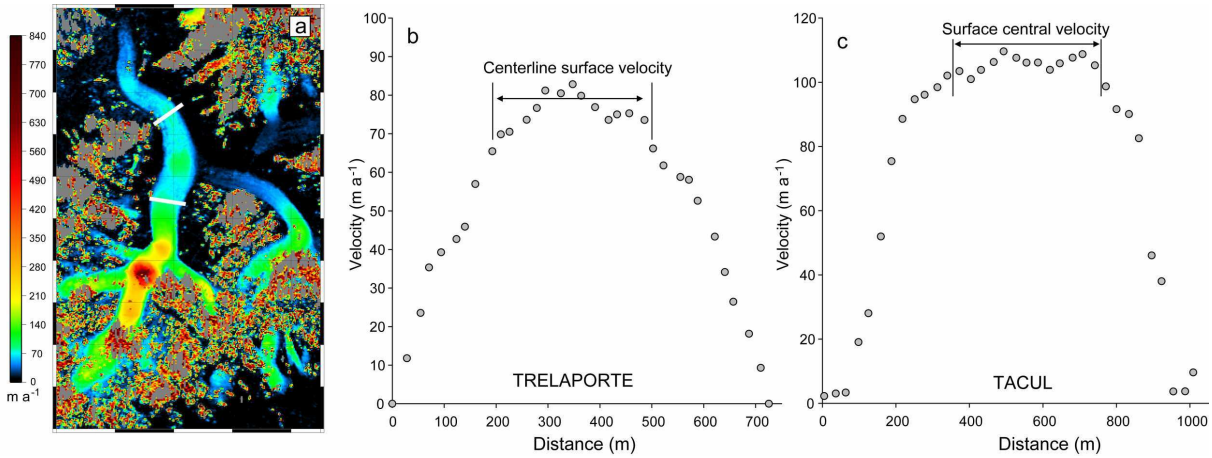

Figure 7: (a) Surface velocity of the Mer de Glace obtained by correlating 2.5 m SPOT5 images acquired 23 August 2003 and 18 September 2003. The thick white line locates the FG_{TAC} and FG_{TRE} cross-sections for which surface velocities are shown on the right (b and c).

Mean cross-section velocities and cross-section areas are multiplied to compute annual ice fluxes. The 1979-2008 mean ice fluxes are 0.0105 km^3 ice a^{-1} at FG_{TRE}. These fluxes, once distributed over a mean downstream glacier area of 1.85 km^2, correspond to an emergence ice velocity of 5.4 m a^{-1}. Between 1979 and 2008, there is a strong reduction of the annual ice fluxes at FG_{TRE}. The minimum ice flux, in 2007-2008, is only 38% of the maximum recorded during hydrological year 1984-1985. Consequently, the emergence ice velocities have decreased from 6.6 m a^{-1} (epoch I) to 4.7 m a^{-1} (epoch II) and 3.8 m a^{-1} (epoch III).

At FG_{TAC}, the 1979-2008 mean ice flux was 0.0230 km^3 ice a^{-1} and also decreased with time: the ice flux in 2007-2008 was 43% of the maximum flux measured during hydrological year 1980-1981. Below FG_{TAC} (feeding an ice-covered area of 4.0 km^2), the emergence ice velocities averaged over 1979-2008 are 5.7 m a^{-1} evolving from 6.7 m a^{-1} (epoch I) to 5.0 m a^{-1} (epoch II) and 4.5 m a^{-1} (epoch III).

4.4. Uncertainties on the ice fluxes

At both cross-sections, the surface topography is known within ±0.5 m (Vincent and others, 2009) and the basal topography within ±10 m (about 5% of the mean cross-section thickness). This uncertainty on the bedrock topography was conservatively adapted from Süsstrunk (1951) who proposed a 3% error for the seismic refraction method. Our findings (see section 5.1) suggest that those ±10 m uncertainties may be too small. The centerline annual velocities are measured in the field with a precision of ±0.2 m a^{-1}. We assumed a ±5 m a^{-1} error (about 5 %) for the conversion of centerline velocities to mean cross-section velocities. After standard propagation of these errors in the ice flux equation (Berthier and others, 2003), the uncertainties vary between ±0.0012 and ±0.0015 km^3 a^{-1} at FG_{TRE}, 11 to 16% of the total ice fluxes. At FG_{TAC}, they vary between ±0.0016 and ±0.0020 km^3 a^{-1}, 10 to 13% of the total ice fluxes.

The uncertainties on the changes in emergence ice velocity from one period to another are ±0.9 to 1.0 m a^{-1} below FG_{TRE}, and are slightly smaller, ±0.6 m a^{-1}, below FG_{TAC}, mainly because the downstream area is twice larger below FG_{TAC}.

5. Discussion

Table 1 and Table 2 list for the two flux gates the annual thinning rates, emergence velocities and surface mass balances for the different epochs and, also, their changes from one epoch to another. Based on these data, we can discuss (i) our ability to close the budget of the thinning and see if the law of mass conservation is respected below each flux gate, (ii) the cause of the accelerated thinning on the Mer de Glace tongue, and (iii) whether reliable changes in surface mass balance could be inferred from changes in geometric variables (ice fluxes and thinning rates) only.

Table 1: Mean annual thinning rate (δh), emergence velocity ($\bar{V}$) and surface mass balances (B) below FG_{TRE} for each epoch and (last column) average values during 1979-2008. The changes from one epoch to another are indicated in italics. The last row contains the sum of the emergence velocity and the surface mass balance. All data in m a^{-1} (ice equivalent).

	1979-94	→	**1994-2000**	→	**2000-2008**	**1979-2008**
δh	-0.6±0.1	*-2.4±0.4*	-3.0±0.3	*-1.0±0.4*	-4.0±0.3	-2.0±0.1
$\bar{V}$	6.7±0.7	*-1.9±1.0*	4.8±0.6	*-0.8±0.9*	4.0±0.6	5.5±0.7
B	-6.8±0.8	*-0.2±0.4*	-7.0±0.9	*-1.0±0.5*	-8.0±1.0	-7.1±0.9
$\bar{V}$+B	-0.1±1.1	*-2.1±1.1*	-2.2±1.1	*-1.8±1.0*	-4.0±1.2	-1.6±1.1

Table 2: Same as Table 1 but for FG_{TAC}.

	1979-94	→	**1994-2000**	→	**2000-2008**	**1979-2008**
δh	-0.8±0.1	*-1.7±0.4*	-2.5±0.3	*-1.0±0.4*	-3.5±0.3	-1.9±0.1
$\bar{V}$	6.6±0.5	*-1.6±0.6*	5.0±0.4	*-0.6±0.6*	4.4±0.4	5.7±0.5
B	-5.6±0.7	*-0.3±0.4*	-5.9±0.8	*-0.9±0.5*	-6.8±0.8	-6.0±0.8
$\bar{V}$+B	1.0±0.9	*-1.9±0.8*	-0.9±0.9	*-1.5±0.8*	-2.4±0.9	-0.3±0.9

5.1. Is the law of mass conservation respected?

If the law of mass conservation was respected, the sum of the emergence velocity and the surface mass balance should equal the thinning rate for each epoch (Table 1 and 2; Figure 8). This is the case within error bars below FG_{TRE} where, if the whole study period (1979-2008) is considered, the mean ice thinning rate is -2.0 m a^{-1}, whereas the sum of emergence ice velocity (5.5 m a^{-1}) and mass balance (-7.1 m a^{-1} ice equivalent) equals -1.6 m a^{-1}. At this cross-section, the law of mass conservation is respected well within error bars for each time period (Figure 8a).

This is a different story at FG_{TAC}, where the sums of the emergence ice velocities and the surface mass balances are systematically larger than the observed ice thinning rates (by 1.7 m a^{-1} in epoch I, 1.6 m a^{-1} in epoch II, 1.1 m a^{-1} in epoch III and 1.6 m a^{-1} overall). Those differences, larger than our uncertainties and similar for the different time periods, indicate that a systematic error affects at least one term of the mass conservation equation. This non closure of the budget of thinning below FG_{TAC} implies that we would make large errors if one term of the mass conservation equation was unknown and inferred from the two others (see section 5.3).

Given the small uncertainties on the thinning rates, this non closure of the mass budget may be explained either by emergence velocities (ultimately ice fluxes at FG_{TAC}) that are too high or

surface mass balances that are not negative enough (or a combination of both). Uncertainties on the tongue-average surface mass balances are large (about ±0.8 m a^{-1} ice equivalent), but to explain the mass budget discrepancy we need a process that decreases the mass balances between FG_{TAC} and FG_{TRE} but not below FG_{TRE}, otherwise we would lose mass conservation below FG_{TRE}. A systematic bias of the mass balance on clean ice (concentrated mainly between FG_{TAC} and FG_{TRE}) could arise from our network of centreline ablation stakes that would not capture some transverse variations in surface mass balance. However, ablations at 7 stakes across the Tacul section were measured between 19 June 2007 and 4 September 2007 and suggest little transverse variations. The 3.5-month mean ablation was 3.55 m w.e. with a standard deviation of 0.2 m w.e., only. Ablations at the two stakes close to the glacier margins did not differ from other measurements. Thus, ablations measured along the centreline are indeed representative of the whole debris-free part of the glacier tongue. Another possibility is that we overestimated the debris-covered area between FG_{TAC} and FG_{TRE} or that the ablation reduction factor under debris (f_d, assumed to be constant) may be lower between FG_{TAC} and FG_{TRE} than below FG_{TRE}. These potential sources of systematic error on the tongue-average mass balance should deserve more attention in the future, for example using the thermal resistance derived from ASTER imagery (Zhang and others, 2011).

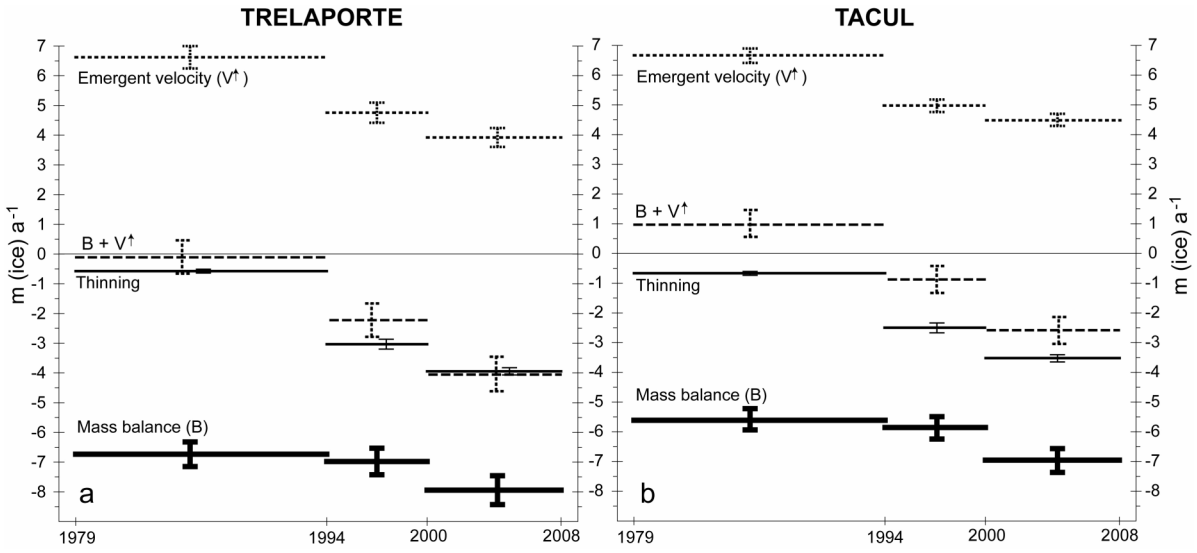

Figure 8: Observed annual thinning rate (thin solid line), emergence velocity ($V^{\uparrow}$, dotted line) and surface mass balance (B, thick solid line) below FG_{TRE} (a) and FG_{TAC} (b) for each epoch. The dashed line represents the sum of the emergence velocity and the surface mass balance ($B+V^{\uparrow}$) and, if mass conservation was respected, should equal the observed thinning rates.

Although the non closure of the mass budget could be partly explain by a systematic error in surface mass balance, an overestimation of the ice fluxes at FG_{TAC} is our preferred hypothesis. If data were available to take into account the ice fluxes from tributary Leschaux Glacier, the total incoming ice fluxes would be increased and the law of mass conservation would be even more violated below FG_{TAC}. The ice fluxes at FG_{TAC} could be lowered (and mass conservation approached but not reached) by decreasing (from 0.9 to 0.8) the factor used to convert surface velocities to mean cross-section velocities. However, a value of 0.8 implies no sliding whereas sliding was found to account for a significant part of the ice flow at this location (Vallon, 1967). Furthermore, we did not find any justification to use a different factor at FG_{TAC} and FG_{TRE}. Thus, our most likely explanation is an overestimated ice thickness at FG_{TAC}. Mass conservation is reached if the ice thickness is reduced by 27%. When this ice thickness correction is applied, the differences between, on one hand, the sum of the ice emergence velocities and the surface mass balances and, one the other hand, the observed ice thinning rates are reduced to 0.0 m a^{-1} in epoch I, 0.2 m a^{-1} in epoch II and -0.1 ice a^{-1} in epoch III. Ice penetrating radar campaigns should

be organized in the future to verify the bedrock topography at FG_{TAC} and validate this hypothesis.

5.2. Budget of the increase in the thinning rate

Within error bars, the budget of the increase in the thinning rate is closed below both cross-sections (Table 1 and 2, Figure 9), i.e. the change in thinning rate from one period to another equals the sum of the changes in surface mass balances and the changes in emergence velocities. The closure is especially good between epoch I and II, partly because the changes in ice thinning rates are large (about 2 m a^{-1}). The agreement is not as satisfactory between epoch II and III with a sum of the changes in surface mass balances and emergence velocities higher than the observed thinning by 83% below FG_{TRE} and 47% below FG_{TAC}. When epoch I and III are compared, those percentages are reduced to, respectively, 14% and 23% suggesting that the changes of ice fluxes and/or ice ablation are slightly overestimated. Below FG_{TAC}, this 23% discrepancy is reduced to only 2% when the ice thickness is diminished by 27%, as proposed in section 5.1 to reach overall mass conservation.

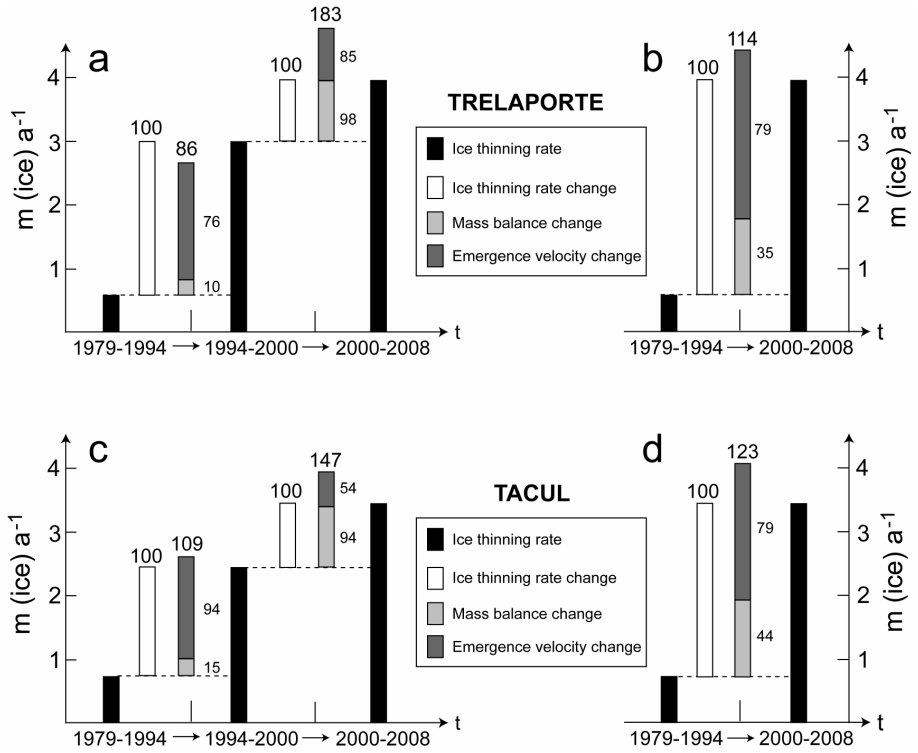

Figure 9: Ice thinning rate (black), its evolution from one period to another (white) and the relative contribution of changes in surface mass balance (light grey) and changes in emergence velocity (dark grey) to the increase in the thinning rate. Upper panels (a, b) are average values below FG_{TRE} whereas lower panels (c, d) are below FG_{TAC}. Numbers close to the histograms correspond to percentage of the change in ice thinning rate. All values in m a^{-1} (ice equivalent).

This relatively good closure of the budget of the increase in the thinning rate at both flux gates gives confidence in our estimates of the relative role played by changes in surface mass balance and ice dynamics. Overall, surface mass balance changes only explained about one third of the increase in the thinning rate. Mass balance changes were very small between epoch I and II but larger between epoch II and III when they explained roughly half of the change in thinning rate (and even two thirds at FG_{TAC}). Decreasing ice fluxes from the upper part of the glacier toward the tongue are responsible for the remaining two thirds of the increase in the thinning rate.

This dynamic response of the Mer de Glace is not an exception given that recent multi-decadal deceleration of glacier tongues seems to be a widespread feature in the Alps (Span and Kuhn, 2003; Vincent and others, 2000; Vincent and others, 2009) and elsewhere (Heid and Kääb, 2011; Kirkbride and Warren, 1999; Nuimura and others, 2011; Zhang and others, 2010). Reduction in the ice fluxes exerts a strong control on the geometry of glaciers by starving their lowest elevations and preserving their upper reaches. The prevalence of this geometric response is confirmed by the observation of limited thinning in the accumulation zone for a large number of glaciers in the European Alps during the last 2-3 decades (Bauder and others, 2007; Berthier and others, 2006; Lambrecht and Kuhn, 2007; Paul and Haeberli, 2008; Span and Kuhn, 2003).

5.3 Can we infer temporal changes in mass balance from changes in thinning rates and ice fluxes?

Given our ability to close the budget of increase in the thinning rate, it seems possible to infer the changes in surface mass balance from the changes in geometric terms (thinning rate and ice flux) only. The rationale for that is that more surface mass balance observations are eagerly desired because changes in surface mass balance are directly related to climate fluctuations but only observed on selected, generally small glaciers, whereas, if bedrock topography had been measured at least once for selected cross-sections, geometric terms (thinning rate and ice flux) could then potentially be derived regularly for large glacier tongues using remote sensing techniques. This strategy would, for example, be particularly relevant to derive tongue-average surface mass balance changes for debris-covered glaciers (e.g., in Himalaya) which are difficult to comprehensively sample in the field due to a rough surface. Indeed, ablation is known to be highly variable on a debris-covered surface and the representativeness of a few ablation stakes is highly questionable (Mihalcea and others, 2006). Furthermore, ablation stakes cannot capture the enhanced ablation taking place at supra-glacial lakes and ice cliffs (Sakai and others, 2000; Sakai and others, 2002). This continuity-equation method has already been applied to glaciers in China (Sakai and others, 2006; Zhang and others, 2010) and, recently, to Khumbu Glacier in Nepal (Nuimura and others, 2011).

Table 3: Comparison of the observed (ΔB_{OBS}) and calculated (ΔB_{CAL}) surface mass balance changes below FG_{TRE} and FG_{TAC} between the different epochs I (1979-1994), II (1994-2000) and III (2000-2008). For FG_{TAC}, we also calculated (last row) the changes in mass balances when the cross section ice thickness is reduced by 27% to respect mass conservation (see section 5.1). All values in m w.e. a^{-1}

		I → II	II → III	I → III
Below FG_{TRE}	ΔB_{OBS}	-0.2±0.4	-0.9±0.4	-1.1±0.4
	ΔB_{CAL}	-0.5±1.0	-0.1±0.9	-0.6±1.0
Below FG_{TAC}	ΔB_{OBS}	-0.2±0.4	-0.9±0.4	-1.1±0.4
	ΔB_{CAL}	-0.1±0.8	-0.4±0.7	-0.5±0.8
	ΔB_{CAL_TUNED}	-0.5±0.8	-0.6±0.7	-1.1±0.8

Our field-observed and calculated changes in surface mass balance for the tongue of the Mer de Glace are given in Table 3. For both cross-sections, they differ on average by 0.3 m w.e. a^{-1} (N=4) and up to 0.8 m w.e. a^{-1}. These differences are expected as they remain within our calculated uncertainties. In the case of FG_{TAC}, a better agreement is reached when the cross-sectional ice thickness is reduced by 27% to respect mass conservation (section 5.1) but still, the sharp increase in ablation between epoch II and III is not fully reproduced. Those discrepancies have the same magnitude as the current climatic signal of mass balance changes and thus, higher accuracy on geometric terms (in particular on the ice fluxes) is required if useful estimates of the changes in mass balance want to be computed on glacier tongues not observed using ablation

stakes. We also stress here the importance of a comprehensive error analysis to determine the reliability of the calculated mass balance changes using this continuity-equation method.

6. Conclusion

In this study, we quantified the geometric and dynamic evolution of the tongue of the Mer de Glace between 1979 and 2008 using an extensive dataset of field and remote sensing observations. Thinning rates were measured by comparing remotely-sensed DEMs calibrated against topographic field surveys. Ice fluxes through two cross-sections were estimated using field-measured annual centreline velocities complemented with satellite-derived velocity fields. Mass balances were observed yearly using ablation stakes and processed using Lliboutry's linear mass balance model to separate their spatial pattern and temporal fluctuations. Those point-wise mass balances were extrapolated to the whole glacier tongue by taking into account the insulating effect of debris, the changes in debris coverage with time and the evolving glacier hypsometry.

Between 1985 and 2008, the whole tongue of the Mer de Glace slowed down (by 51% at FG_{TAC} and 53% at FG_{TRE}) and thinned (by 17% at FG_{TAC} and 23% at FG_{TRE}) so that the annual ice fluxes were reduced by about 60%. Meanwhile, area-average ablation increased by 1.2 m w.e. a^{-1}. Positive (lowering of the glacier surface) and negative (loss of low lying areas close to the front and growth of debris-covered areas) ablation feedbacks nearly cancelled out.

Because all three terms of the continuity equation were estimated independently we could verify the correct closure of the mass budget for the glacier tongue below FG_{TRE}. Conversely, its non-closure below FG_{TAC} suggests that the ice fluxes through this gate may be overestimated, possibly due to errors on the bedrock topography. Future field campaigns should aim at verifying the ice thickness at this location. However, we cannot rule out a systematic error in the surface mass balance between FG_{TAC} and FG_{TRE} due to the unknown thickness of the evolving debris cover.

Our analysis reveals that more than two thirds of the increase in the thinning rate for the lower Mer de Glace is due to decreasing ice fluxes from the upper parts of the glacier and only one third due to rising ice ablation. Thus, we quantitatively confirm here the obvious need to take into account ice dynamics and its continuous change with time to understand the reaction of mountain glacier tongues to climate change.

Our extensive dataset also allow evaluation of the continuity-equation method of determining the temporal evolution of the surface mass balance for a whole glacier tongue. Errors on the geometric terms (ice fluxes and thinning rates) in the continuity equation indicate some uncertainties of 0.8 to 1 m w.e. a^{-1} for the changes in mass balance for the tongue of the Mer de Glace. These large *a priori* errors are confirmed by the comparison of the calculated values to field-observed mass balance changes that indicates errors up to 0.8 m w.e. a^{-1}. These errors have the same magnitude as the recent mass balance response to climate change, severely limiting the current usefulness of this continuity-equation method. Nearly an order of magnitude needs to be gained on our ability to measure the geometric terms (in particular the ice fluxes) from space before this method can be usefully applied to remote and large mountain glaciers. Thus, although remote sensing techniques have reached a certain level of maturity to observe velocity fields or glacier-wide averaged mass balances, dense networks of ablation stakes on selected glaciers seem to remain the best mean to assess the spatial pattern and temporal changes in their mass balance, and thus, the influence of climate change.

7. Acknowledgements

We thank Romain Dolques for his early work on the 2008 SPOT5 DEM. We thank all those who have taken part in collecting the extensive field measurements on the Mer de Glace. Yves Arnaud and Frédérique Rémy are acknowledged for early discussions on those mass budget analyses. This study has been funded by the French Space Agency (CNES) through the TOSCA and ISIS proposal #97, the Programme National de Télédétection Spatiale (PNTS), the Observatoire des Sciences de l'Univers de Grenoble (OSUG) and by the Institut National des Sciences de l'Univers (INSU). Part of the field data used in this paper is available through the Glacioclim-Alp website (http://www-lgge.obs.ujf-grenoble.fr/ServiceObs/index.htm). Constructive comments by two anonymous referees improved our manuscript.

8. References

Arnold, N.S., W.G. Rees, A.J. Hodson and J. Kohler. 2006. Topographic controls on the surface energy balance of a high Arctic valley glacier. *Journal of Geophysical Research - Earth Surface*, **111**(F02011).

Bauder, A., M. Funk and M. Huss. 2007. Ice-volume changes of selected glaciers in the Swiss Alps since the end of the 19th century. *Annals of Glaciology*, **46**, 145-149.

Berthier, E., B. Raup and T. Scambos. 2003. New velocity map and mass-balance estimate of Mertz Glacier, East Antarctica, derived from Landsat sequential imagery. *Journal of Glaciology*, **49**(167), 503-511.

Berthier, E., Y. Arnaud, D. Baratoux, C. Vincent and F. Remy. 2004. Recent rapid thinning of the "Mer de Glace" glacier derived from satellite optical images. *Geophysical Research Letters*, **31**(17), L17401.

Berthier, E. *and others*. 2005. Surface motion of mountain glaciers derived from satellite optical imagery. *Remote Sensing of Environment*, **95**(1), 14-28.

Berthier, E., Y. Arnaud, C. Vincent and F. Remy. 2006. Biases of SRTM in high-mountain areas: Implications for the monitoring of glacier volume changes. *Geophysical Research Letters*, **33**(8), L08502.

Berthier, E. 2007. Dynamique et bilan de masse des glaciers de montagne (Alpes, Islande, Himalaya). Contribution de l'imagerie satellitaire. *La Houille Blanche*, **02**, 116-121.

Berthier, E., E. Schiefer, G.K.C. Clarke, B. Menounos and F. Remy. 2010. Contribution of Alaskan glaciers to sea level rise derived from satellite imagery. *Nature Geoscience*, **3**(2), 92-95.

Cuffey, K.M. and W.S.B. Paterson, 2010. The physics of glaciers. Academic Press Inc, Amsterdam.

Deline, P. 2005. Change in surface debris cover on Mont Blanc massif glaciers after the 'Little Ice Age' termination. *Holocene*, **15**(2), 302-309.

Dyurgerov, M.B. and M.F. Meier. 1999. Analysis of winter and summer glacier mass balances. *Geografiska Annaler Series a-Physical Geography*, **81A**(4), 541-554.

Elsberg, D.H., W.D. Harrison, K.A. Echelmeyer and R.M. Krimmel. 2001. Quantifying the effects of climate and surface change on glacier mass balance. *Journal of Glaciology*, **47**(159), 649-658.

Gluck, S. 1967. Détermination du lit rocheux sous la Mer de Glace par séismique-réflexion. *Comptes Rendus De L'Academie Des Sciences*, **264**(19), 2272-2275.

Gudmundsson, G.H. and A. Bauder. 1999. Towards an indirect determination of the mass-balance distribution of glaciers using the kinematic boundary condition. *Geografiska Annaler Series a-Physical Geography*, **81A**(4), 575-583.

Hagen, J.O., T. Eiken, J. Kohler and K. Melvold. 2005. Geometry changes on Svalbard glaciers: mass-balance or dynamic response? *Annals of Glaciology*, **42**, 255-261.

Heid, T. and A. Kääb. 2011. Worldwide widespread decadal-scale decrease of glacier speed revealed using repeat optical satellite images. *The Cryosphere Discussion*, **5**, 3025-3051.

Hubbard, A. *and others*. 2000. Glacier mass-balance determination by remote sensing and high-resolution modelling. *Journal of Glaciology*, **46**(154), 491-498.

Huss, M., S. Sugiyama, A. Bauder and M. Funk. 2007. Retreat scenarios of Unteraargletscher, Switzerland, using a combined ice-flow mass-balance model. *Arctic, Antarctic, and Alpine Research*, **39**(3), 422-431.

Huss, M., A. Bauder, M. Funk and R. Hock. 2008. Determination of the seasonal mass balance of four Alpine glaciers since 1865. *Journal of Geophysical Research-Earth Surface*, **113**(F1).

Kääb, A. and M. Funk. 1999. Modelling mass balance using photogrammetric and geophysical data: a pilot study at Griesgletscher, Swiss Alps. *Journal of Glaciology*, **45**(151), 575-583.

Kääb, A. 2000. Photogrammetric reconstruction of glacier mass balance using a kinematic ice-flow model: a 20 year time series on Grubengletscher, Swiss Alps. *Annals of Glaciology*, **31**, 45-52.

Kirkbride, M.P. and C.R. Warren. 1999. Tasman Glacier, New Zealand: 20th-century thinning and predicted calving retreat. *Global and Planetary Change*, **22**(1-4), 11-28.

Kohler, J. *and others*. 2007. Acceleration in thinning rate on western Svalbard glaciers. *Geophysical Research Letters*, **34**(L18502).

Lambrecht, A. and M. Kuhn. 2007. Glacier changes in the Austrian Alps during the last three decades, derived from the new Austrian glacier inventory. *Annals of Glaciology*, **46**, 177-184.

Lemke, P. *and others*, 2007. Observations: Changes in Snow, Ice and Frozen Ground. In: S. Solomon et al. (Editors), *Climate Change 2007: The Physical Science Basis. Contribution of Working Group I to the Fourth Assessment Report of the Intergovernmental Panel on Climate Change,* Vol. Cambridge University Press, Cambridge, United Kingdom and New York, NY, USA, pp. 337-383.

Lliboutry, L. 1974. Multivariate statistical analysis of glacier annual balances. *Journal of Glaciology*, **13**, 371-392.

Lliboutry, L. and L. Reynaud. 1981. "Global dynamics" of a temperate valley glacier, Mer de Glace, and past velocities deduced from Forbes bands. *Journal of Glaciology*, **27**(96), 207-226.

Magnússon, E., H. Björnsson, J. Dall and F. Palsson. 2005. Volume changes of Vatnajokull ice cap, Iceland, due to surface mass balance, ice flow, and subglacial melting at geothermal areas. *Geophysical Research Letters*, **32**(5).

Mihalcea, C., C. Mayer, G. Diolaiuti, A. Lambrecht, C. Smiraglia and G. Tartari. 2006. Ice ablation and meteorolopical conditions on the debris-covered area of Baltoro glacier, Karakoram, Pakistan. *Annals of Glaciology*, **43**, 292-300.

Nuimura, T., K. Fujita, K. Fukui, K. Asahi, R. Aryal and Y. Ageta. 2011. Temporal changes in elevation of the debris-covered ablation area of Khumbu Glacier in the Nepal Himalaya since 1978. *Arctic, Antarctic, and Alpine Research*, **43**(2), 246-255.

Nuth, C., G. Moholdt, J. Kohler, J.O. Hagen and A. Kääb. 2010. Svalbard glacier elevation changes and contribution to sea level rise. *Journal of Geophysical Research-Earth Surface*, **115**, F01008.

Nuth, C., T.V. Schuler, J. Kohler, B. Altema and J.O. Hagen. 2012. Estimating the long-term calving flux of Kronebreen, Svalbard, from geodetic elevation changes and mass-balance modelling. *Journal of Glaciology*, **58**(207), 119–133.

Oerlemans, J., 2001. Glaciers and climate change. A. A. Balkema Publishers, Rotterdam.

Oerlemans, J., R.H. Giesen and M.R. Van den Broeke. 2009. Retreating alpine glaciers: increased melt rates due to accumulation of dust (Vadret da Morteratsch, Switzerland). *Journal of Glaciology*, **55**(192), 729-736.

Ohmura, A. 2006. Changes in mountain glaciers and ice caps during the 20th century. *Annals of Glaciology*, **43**, 361-368.

Paul, F., A. Kääb and W. Haeberli. 2007. Recent glacier changes in the Alps observed by satellite: consequences for future monitoring strategies. *Global and Planetary Change*, **56**, 111-122.

Paul, F. and W. Haeberli. 2008. Spatial variability of glacier elevation changes in the Swiss Alps obtained from two digital elevation models. *Geophysical Research Letters*, **35**, L21502.

Rabatel, A., J.-P. Dedieu and C. Vincent. 2005. Using remote-sensing data to determine equilibrium-line altitude and mass-balance time series: validation on three French glaciers, 1994-2002. *Journal of Glaciology*, **51**(175), 539-546.

Raymond, C.F. 1971. Flow in a transverse section of Athabasca Glacier, Alberta. *Journal of Glaciology*, **10**(58), 55-84.

Reynaud, L., 1973. Etude de la dynamique des séracs du Géant (Massif du Mont-Blanc). PhD Thesis, Université Scientifique et Médicale, Grenoble.

Reynaud, L., M. Vallon and A. Letreguilly. 1986. Mass-balance measurements: problems and two news methods of determining variations. *Journal of Glaciology*, **32**(112).

Rignot, E., A. Rivera and G. Casassa. 2003. Contribution of the Patagonia Icefields of South America to sea level rise. *Science*, **302**(5644), 434-437.

Sakai, A., N. Takeuchi, K. Fujita and M. Nakawo, 2000. Role of supraglacial ponds in the ablation process of a debris-covered glacier in the Nepal Himalayas. In: M. Nakawo, C.F. Raymond and A. Fountain (Editors), Debris-covered glaciers. International Association of Hydrological Sciences, Seattle, pp. 119-130.

Sakai, A., M. Nakawo and K. Fujita. 2002. Distribution characteristics and energy balance of ice cliffs on debris-covered glaciers, Nepal Himalaya. *Arctic Antarctic and Alpine Research*, **34**(1), 12-19.

Sakai, A., K. Fujita, K. Duan, J. Pu, M. Nakawo and T. Yao. 2006. Five decades of shrinkage of July 1st glacier, Qilian Shan, China. *Journal of Glaciology*, **52**(176), 11-16.

Schwitter, M.P. and C.F. Raymond. 1993. Changes in the Longitudinal Profiles of Glaciers during Advance and Retreat. *Journal of Glaciology*, **39**(133), 582-590.

Soruco, A., C. Vincent, B. Francou and J.F. Gonzalez. 2009. Glacier decline between 1963 and 2006 in the Cordillera Real, Bolivia. *Geophysical Research Letters*, **36**.

Span, N. and M. Kuhn. 2003. Simulating annual glacier flow with a linear reservoir model. *Journal of Geophysical Research-Atmospheres*, **108**(D10).

Surazakov, A.B. and V.B. Aizen. 2006. Estimating volume change of mountain glaciers using SRTM and map-based topographic data. *IEEE Transactions on Geoscience and Remote Sensing*, **44**(10), 2991-2995.

Süsstrunk, A. 1951. Sondage du glacier par la méthode sismique. *La Houille Blanche*, **A**, 309-319.

Thibert, E. and C. Vincent. 2009. Best possible estimation of mass balance combining glaciological and geodetic methods. *Annals of Glaciology*, **50**(50), 112-118.

Vallon, M. 1961. Epaisseur du glacier du Tacul (Massif du Mont-Blanc). *Comptes Rendus De L'Academie Des Sciences*, **252**(12), 1815-1817.

Vallon, M., 1967. Contribution à l'étude de la Mer de Glace. PhD Thesis, Facultés des sciences de Grenoble, 72 pp.

Vincent, C. 1999. Etude du glacier de la Mer de Glace. Rapport d'étude pour la Compagnie du Mont Blanc.

Vincent, C., M. Vallon, L. Reynaud and E. Le Meur. 2000. Dynamic behaviour analysis of glacier de Saint Sorlin, France, from 40 years of observations, 1957-97. *Journal of Glaciology*, **46**(154), 499-506.

Vincent, C. 2002. Influence of climate change over the 20th Century on four French glacier mass balances. *Journal of Geophysical Research-Atmospheres*, **107**(D19).

Vincent, C., G. Kappenberger, F. Valla, A. Bauder, M. Funk and E. Le Meur. 2004. Ice ablation as evidence of climate change in the Alps over the 20th century. *Journal of Geophysical Research-Atmospheres*, **109**(D10).

Vincent, C., E. Le Meur, D. Six and E. Thibert. 2007. Un service d'observation des glaciers des alpes françaises« glacioclim-alpes », pour quoi faire ? *La Houille Blanche*, **03**, 86-95.

Vincent, C., A. Soruco, D. Six and E. Le Meur. 2009. Glacier thickening and decay analysis from 50 years of glaciological observations performed on Glacier d'Argentière, Mont Blanc area, France. *Annals of Glaciology*, **50**(50), 73–79.

Willis, I.C. 1995. Intra-annual variations in glacier motion: a review. *Progress in Physical Geography*, **19**(1), 61-106.

Zhang, Y., K. Fujita, S.Y. Liu, Q.A. Liu and X. Wang. 2010. Multi-decadal ice-velocity and elevation changes of a monsoonal maritime glacier: Hailuogou glacier, China. *Journal of Glaciology*, **56**(195), 65-74.

Zhang, Y., K. Fujita, S. Liu, Q. Liu and T. Nuimura. 2011. Distribution of debris thickness and its effect on ice melt at Hailuogou glacier, southeastern Tibetan Plateau, using in situ surveys and ASTER imagery. *Journal of Glaciology*, **57**(206), 1147–1157.

Zumbühl, H.J., D. Steiner and S.U. Nussbaumer. 2008. 19th century glacier representations and fluctuations in the central and western European Alps: An interdisciplinary approach. *Global and Planetary Change*, **60**(1-2), 42-57.